

# Absence of Anderson localization of light in a random ensemble of point scatterers

S.E. Skipetrov<sup>1,\*</sup> and I.M. Sokolov<sup>2,†</sup>

<sup>1</sup>*Université Grenoble 1/CNRS, LPMCM UMR 5493, B.P. 166, 38042 Grenoble, France*

<sup>2</sup>*Department of Theoretical Physics, State Polytechnic University, 195251 St. Petersburg, Russia*  
(Dated: March 20, 2013)

As discovered by Philip Anderson in 1958, strong disorder can block propagation of waves and lead to the localization of wave-like excitations in space. Anderson localization of light is particularly exciting in view of its possible applications for random lasing or quantum information processing. We show that in contradiction to the common belief, Anderson localization of light cannot be achieved in a random three-dimensional ensemble of point scattering centers that is a paradigm model to study multiple scattering of waves. This suggests that fully disordered systems are not suitable for observation of Anderson localization of light and casts doubt on the very possibility of this phenomenon for light in any three-dimensional medium without sufficient structural correlations.

Anderson localization—the appearance and dominance of localized states in strongly disordered systems—is believed to be a universal phenomenon for all quantum and classical waves [1–3]. In particular, three-dimensional (3D) disordered systems are expected to exhibit a transition from the “metallic” phase with extended states to the “insulating” one with localized states, upon increasing the disorder. This transition was observed for electrons in disordered solids [4], ultrasound [5], and cold atoms [6–8]. Reports of Anderson localization of light in 3D also exist [9–11]. Here we present a theoretical study of light scattering in a 3D ensemble of resonant point scatterers (atoms) at random positions. We show that Anderson localization takes place only in the scalar approximation and disappears when polarization effects are taken into account. Resonant point scatterers allow for the strongest overall scattering thanks to the combination of a large scattering crosssection and the possibility to pack an arbitrary large number of scatterers in a finite volume. Therefore, our results question the very possibility of Anderson localization of light in any 3D random medium, at least as far as there are no correlations in scatterer positions.

Samples used in experiments on Anderson localization of light—semiconductor [9, 12] or dielectric [10, 11] powders, porous semiconductors [13], or disordered photonic crystals [14]—are complex photonic media that do not allow for accurate theoretical description of light scattering. Instead, theoretical physicists like to work with a simpler model, an ensemble of point scatterers, and implicitly assume that the overall transport properties of large disordered samples are independent of their microscopic details. Such an approach can indeed be quite successful and allows for a good understanding of underlying physics [15, 16]. In addition, the point-scatterer approximation is excellent for description of light scattering on ensembles of cold atoms which therefore provide a fantastic and practically realizable playground for testing the theory [17].

Let us apply the point-scatterer model to study Anderson localization of light and try to go as far as possible

without additional approximations. For concreteness, we assume that the point scatterers are two-level atoms each having a non-degenerate ground state  $|g\rangle$  with energy  $E_g$  and the total angular momentum  $J_g = 0$  and an excited state  $|e\rangle$  with  $E_e = E_g + \hbar\omega_0$ ,  $J_e = 1$ , and lifetime  $1/\Gamma_0$  ( $\hbar$  is the Planck’s constant). The excited state is thus triply degenerate and splits in 3 sub-states with different projections  $m = -1, 0, 1$  of the angular momentum  $\mathbf{J}_e$  on the quantization axis  $z$ . To study light scattering in a random ensemble of identical atoms, we start with microscopic quantum-mechanical equations that describe the joint dynamics of operators corresponding to the atoms and to the electromagnetic field [18–20]. These equations are solved for the field variables and equations for atomic operators are obtained in which coupling between atoms is described by the so-called “Green’s matrix”  $G$ . It is essentially built up of Green’s functions of Maxwell equations, describing propagation of light from one atom to another.  $G$  is a  $3N \times 3N$  random matrix of which a particular realization is determined by the ensemble of random positions  $\{\mathbf{r}_i\}$  of  $N$  atoms in 3D Euclidean space [18, 19]:

$$G_{e_i e_j} = i\delta_{e_i e_j} - \frac{2}{\Gamma_0} (1 - \delta_{e_i e_j}) \sum_{\mu, \nu} d_{e_i g_i}^\mu d_{g_j e_j}^\nu \frac{e^{ik_0 r_{ij}}}{\hbar r_{ij}^3} \times \left\{ \delta_{\mu\nu} [1 - ik_0 r_{ij} - (k_0 r_{ij})^2] - \frac{r_{ij}^\mu r_{ij}^\nu}{r_{ij}^2} [3 - 3ik_0 r_{ij} - (k_0 r_{ij})^2] \right\}. \quad (1)$$

Here  $\mathbf{d}_{e_i g_i}$  is the dipole moment operator of the transition  $|g\rangle \rightarrow |e\rangle$  of the atom  $i$ ,  $\mathbf{r}_{ij} = \mathbf{r}_i - \mathbf{r}_j$ , and  $k_0 = \omega_0/c$ , with  $c$  the vacuum speed of light. The superscripts  $\mu$  and  $\nu$  denote projections of vectors on axes of the reference frame.

Any excitation of the ensemble of  $N$  atoms coupled through the electromagnetic field can be expanded over eigenvectors  $\psi_n$  of the matrix  $G$ . The real and imaginary parts of its eigenvalues  $\Lambda_n$  yield the frequencies  $\omega_n = \omega_0 - (\Gamma_0/2)\text{Re}\Lambda_n$  and decay rates  $\Gamma_n/2 = (\Gamma_0/2)\text{Im}\Lambda_n$  of

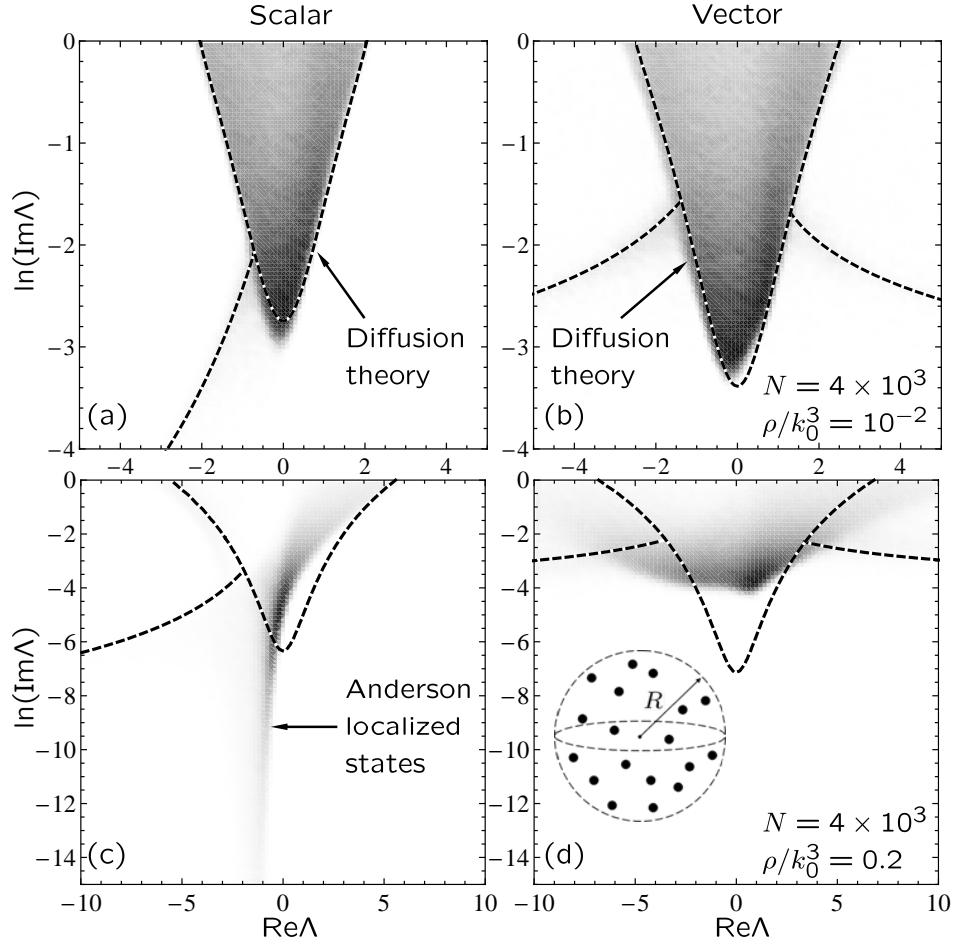


FIG. 1. Density of eigenvalues of the random Green's matrix. Grayscale density plots of the probability density  $p(\Lambda)$  for  $\Lambda$ 's corresponding to long-lived states ( $\text{Im}\Lambda < 1$ ). Dashed lines show the border of the eigenvalue domain following from the diffusion theory and the spiral branches along which eigenvalues corresponding to subradiant states are concentrated [20, 21]. Panels (a) and (b) correspond to a low density at which the majority of eigenvalues are contained within the boundary imposed by the diffusion theory. Panels (c) and (d) correspond to a high density, for which states with very small decay rates  $\text{Im}\Lambda$  appear in the scalar model, but not in the vector one. The smallest  $\text{Im}\Lambda$  of the vector model is even larger than the prediction of the diffusion theory. The inset of panel (d) shows  $N$  atoms (black dots) randomly distributed in a sphere of radius  $R$ .

the corresponding eigenstates.  $G$  is therefore the fundamental object to study in order to understand the behavior of collective excitations in the atomic ensemble. We will be interested in the spatial localization of  $\psi_n$  and will compare the properties of the matrix (1) that takes into account the vector character of light with those of its scalar approximation

$$G_{e_i e_j} = i\delta_{e_i e_j} + (1 - \delta_{e_i e_j}) \frac{e^{ik_0 r_{ij}}}{k_0 r_{ij}} \quad (2)$$

that is often used to further simplify the problem [21, 22]. Indeed, it is generally believed that the vector nature of light does not significantly modify the main features of the Anderson localization problem [23–25]. Previous studies of matrices similar to (1) and (2) supported this point of view [26–28]. The results that we present below show, however, that it is wrong for light scattering in an

ensemble of point scatterers.

We first analyze the density of eigenvalues  $\Lambda$  of the Green's matrices (1) and (2) with a particular attention paid to the part of the spectrum corresponding to long-lived states with  $\text{Im}\Lambda < 1$ . Random realizations of Green's matrices (1) and (2) were generated by randomly choosing  $N$  points in a sphere of radius  $R$  and volume  $V$  [see the inset of Fig. 1(d)]. Their eigenvalues  $\Lambda_n$  and eigenvectors  $\psi_n = \{\psi_{ne_i}\}$  obeying  $G\psi_n = \Lambda_n\psi_n$  were computed using MATLAB or FORTRAN codes. Averaging was performed over 120 and 75 realizations for the scalar model, and over 40 and 25 realizations for the vector model, at  $N = 2 \times 10^3$  and  $4 \times 10^3$ , respectively. In the scalar case, similar results were obtained for  $N$  up to  $10^4$ . The density of eigenvalues  $\Lambda$  for  $N = 4 \times 10^3$  is shown in Fig. 1. At low densities  $\rho = N/V$ , the results obtained for scalar and vector models are similar, most of

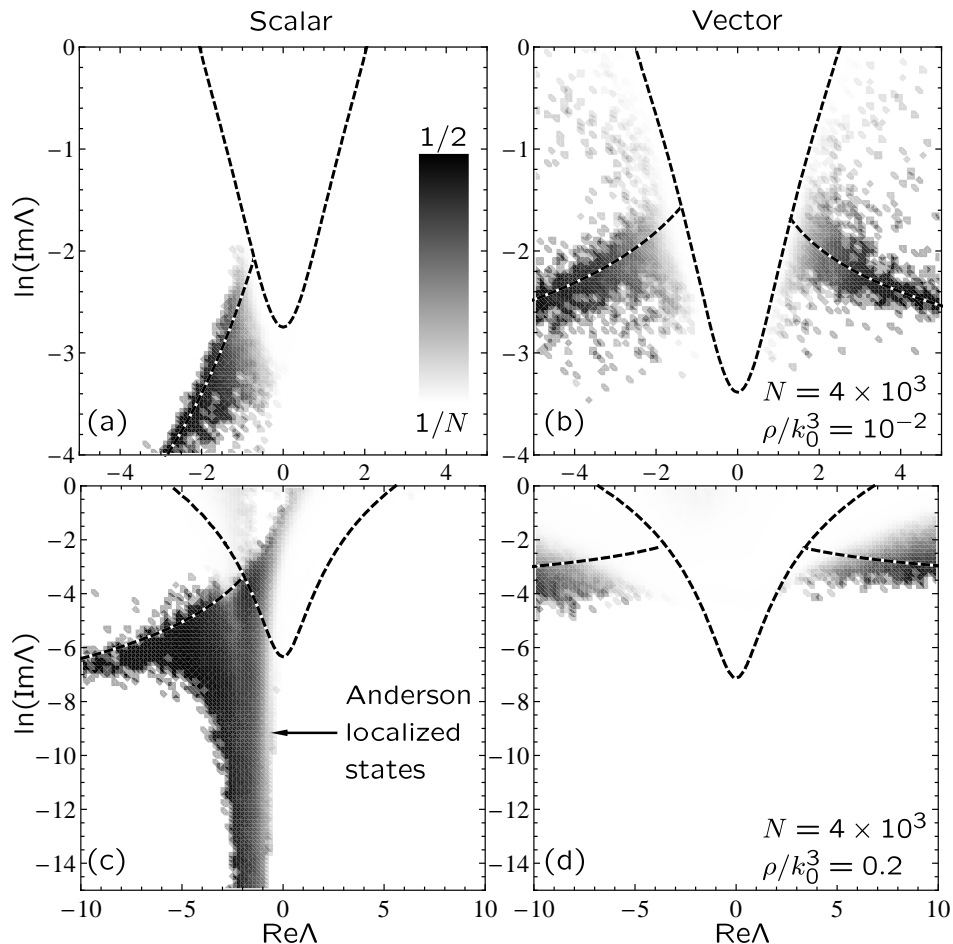


FIG. 2. Inverse participation ratio of eigenvectors. Grayscale density plot of the average inverse participation ratio (IPR) as a function of the eigenvalue  $\Lambda$  of the corresponding eigenvector. Dashed lines are the same as in Fig. 1. At low density, subradiant states localized on pairs of closely located scatterers exist in both scalar (a) and vector (b) models. These states have  $\text{IPR} \simeq 1/2$ . At high density, Anderson-localized states with large IPR appear in the scalar model (c), but not in the vector one (d).

the eigenvalues being restricted to a region delimited by a line following from the diffusion theory of light scattering [20, 21]. At densities exceeding  $\rho/k_0^3 \approx 0.1$ , however, we observe that in the scalar model, a significant fraction of eigenvalues cross this line and acquire very small decay rates  $\text{Im}\Lambda$ . No such long-lived states appear in the vector model.

To test the intuitive conjecture that the long-lived states corresponding to eigenvalues with small imaginary parts may be localized in space, we show in Fig. 2 maps of the average inverse participation ratio (IPR) for the same parameters as in Fig. 1.  $\text{IPR}_n = \sum_{i=1}^N |\psi_n(\mathbf{r}_i)|^4 / (\sum_{i=1}^N |\psi_n(\mathbf{r}_i)|^2)^2$  quantifies the degree of spatial localization of the eigenvector  $\psi_n$ . It is of order  $1/M$  for an eigenvector localized on  $M$  atoms. In the vector model, each  $\psi_n(\mathbf{r}_i)$  is a vector with 3 components and  $|\psi_n(\mathbf{r}_i)|$  should be understood as its length. As we see from Fig. 2, states localized on a small number of atoms exist even

at small densities. They are typically localized on pairs of very closely located atoms and are due to the phenomenon of subradiance that does not require multiple scattering and therefore has nothing to do with Anderson localization [20–22]. Their eigenvalues are concentrated along the dashed lines that depict the evolution of the smallest eigenvalue of a  $2 \times 2$  Green's matrix as the distance between the two atoms is varied. In the scalar model, however, localized states of a different type appear at densities larger than  $\rho/k_0^3 \approx 0.1$ . These states have very small decay rates, in agreement with Fig. 1. Once again, no such localized states are seen in the vector case.

To convince ourselves that the localized states appearing at large densities in the scalar model are due to Anderson localization, we perform the scaling analysis [29]. We compute the average dimensionless lifetime of eigenstates  $\langle 1/\text{Im}\Lambda \rangle = \delta\omega^{-1}$  and the average spacing of nearest dimensionless eigenfrequencies  $\Delta\omega =$

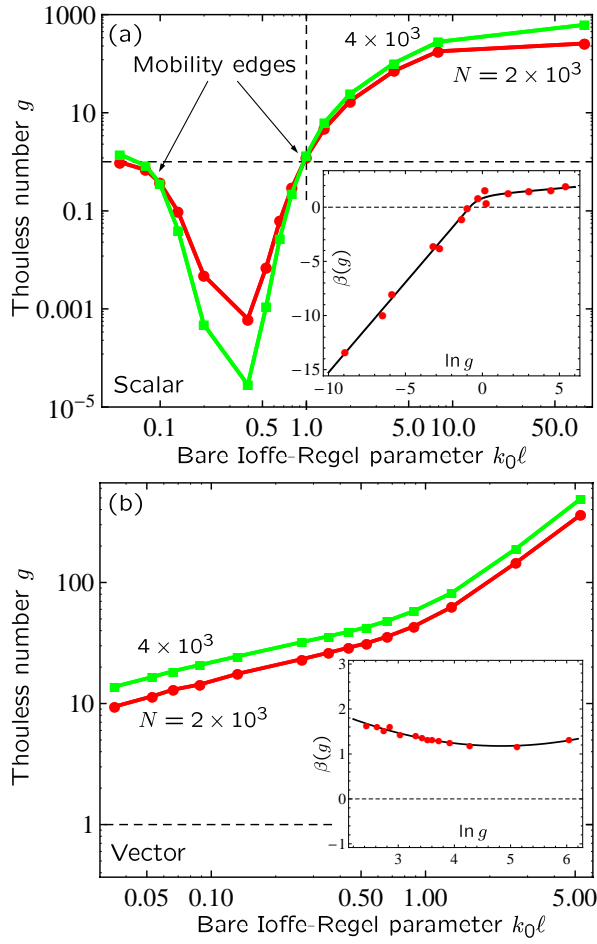


FIG. 3. Scaling in scalar and vector models. (a) Thouless number  $g$  as a function of the bare Ioffe-Regel parameter  $k_0\ell$  for the scalar model at frequency  $\omega = \omega_0 + \Gamma_0/2$  and  $N = 2 \times 10^3$  (circles) and  $4 \times 10^3$  (squares). The curves cross at  $g \approx k_0\ell \approx 1$  and then again at  $k_0\ell \ll 1$  and  $g \approx 1$ . Localization transitions take place at these points, as confirmed by the analysis of the scaling function  $\beta(g)$  shown in the inset that changes sign at  $g \approx 1$  (circles). (b) The same for the vector model. Solid lines in the insets are guides for the eye.

$\langle \text{Re}\Lambda_n - \text{Re}\Lambda_{n-1} \rangle$  for eigenvalues  $\Lambda_n$  in a strip of unit width around  $\text{Re}\Lambda = -1$  where, according to Figs. 1 and 2, the localization effects are important in the scalar model. The localization transition for light at frequency  $\omega = \omega_0 + \Gamma_0/2$  is expected to take place when the Thouless number  $g = \delta\omega/\Delta\omega$  becomes of order unity [29, 30]. In Fig. 3 we show  $g$  as a function of the bare Ioffe-Regel parameter  $k_0\ell$ , with the on-resonance mean free path  $\ell$  calculated in the independent-scattering approximation (ISA) [15]:  $\ell = k_0^2/4\pi\rho$  for the scalar and  $\ell = k_0^2/6\pi\rho$  for the vector model, respectively. In the scalar case, the curves  $g(k_0\ell)$  corresponding to different  $N$  cross at  $g \approx 1$ ,  $k_0\ell \approx 1$ , as expected from the Thouless and Ioffe-Regel criteria of localization [2]. A second crossing takes place at much smaller  $k_0\ell$  (corresponding to a very large density  $\rho$  at which ISA is not a good approx-

imation for  $\ell$ ) and signals the disappearance of localization; the system starts to approach the effective medium regime. A finite-difference estimate of the scaling function  $\beta(g) = \partial \ln g / \partial \ln k_0 R$  obtained from the data of the main plot is shown in the inset of Fig. 3(a). As expected,  $\beta(g)$  changes sign at  $g \approx 1$ , confirming Anderson transition in the scalar model. However, none of the above signatures of Anderson localization is seen in Fig. 3(b) where we present the results for the vector model.  $g(k_0\ell)$  corresponding to different  $N$  do not cross,  $g$  always remains larger than 1, and  $\beta(g) > 0$  does not change sign, suggesting no localization transition.

Our discovery of the absence of Anderson localization of light in a 3D random ensemble of point scatterers shows that completely random systems (such as, e.g., clouds of cold atoms) are not suitable for observation of this phenomenon. It also partially explains the rareness of its experimental realizations and indirectly supports the ideas about the importance of correlations in positions of scatterers (e.g., partial order) for achieving Anderson localization of light [25]. However, it remains to be seen if such correlations, either long- or short-range, may induce localization. The model presented in this work is perfectly suitable for such a study.

SES thanks A. Goetschy for fruitful discussions. This work was supported by the Federal Program for Scientific and Scientific-Pedagogical Personnel of Innovative Russia for 2009–2013 (contract No. 14.B37.21.1938).

\* Sergey.Skipetrov@grenoble.cnrs.fr

† igor.m.sokolov@gmail.com

- [1] P.W. Anderson, *Phys. Rev.* **109**, 1492 (1958).
- [2] A. Lagendijk, B.A. van Tiggelen, and D.S. Wiersma, *Phys. Today* **62**(8), 24 (2009).
- [3] E. Abrahams, Ed., *50 Years of Anderson Localization* (World Scientific, Singapore, 2010).
- [4] For a review of experiments see R.C. Dynes, Localization and the metalinsulator transition—experimental observations, in Ref. [3], pp. 213–230.
- [5] H. Hu, A. Strybulevych, J.H. Page, S.E. Skipetrov, and B.A. van Tiggelen, *Nature Phys.* **4**, 945 (2008).
- [6] J. Chabé *et al.*, *Phys. Rev. Lett.* **101**, 255702 (2008).
- [7] S.S. Kondov, W.R. McGehee, J.J. Zirbel, and B. DeMarco, *Science* **333**, 66 (2011).
- [8] F. Jendrzejewski *et al.*, *Nature Phys.* **8**, 398 (2012).
- [9] D.S. Wiersma, P. Bartolini, A. Lagendijk, and R. Righini, *Nature* **390**, 671 (1997).
- [10] M. Störzer, P. Gross, C.M. Aegerter, and G. Maret, *Phys. Rev. Lett.* **96**, 063904 (2006).
- [11] T. Sperling, W. Bührer, C.M. Aegerter, and G. Maret, *Nature Photon.* **7**, 48 (2013).
- [12] T. van der Beek, P. Barthelemy, P.M. Johnson, D.S. Wiersma, and A. Lagendijk, *Phys. Rev. B* **85**, 115401 (2012).
- [13] F.J.P. Schuurmans, M. Megens, D. Vanmaekelbergh, and A. Lagendijk, *Phys. Rev. Lett.* **83**, 2183 (1999).

- [14] K.M. Douglass, S. John, T. Suezaki, G.A. Ozin, and A. Dogariu, *Opt. Exp.* **19**, 25320 (2011).
- [15] A. Lagendijk and B.A. van Tiggelen, *Phys. Rep.* **270**, 143 (1996).
- [16] P. De Vries, D.V. van Coevorden, and A. Lagendijk, *Rev. Mod. Phys.* **70**, 447 (1998).
- [17] R. Kaiser, in *Diffuse Waves in Complex Media*, J.-P. Fouque, Ed. (Kluwer, Dordrecht, 1999).
- [18] Ya.A. Fofanov, A.S. Kuraptsev, I.M. Sokolov, and M.D. Havey, *Phys. Rev. A* **84**, 053811 (2011).
- [19] I.M. Sokolov, D.V. Kupriyanov, and M.D. Havey, *J. Exp. Theor. Phys.* **112**, 246 (2011).
- [20] A. Goetschy, *Light in Disordered Atomic Systems: Euclidean Matrix Theory of Random Lasing*. Ph.D. thesis (J. Fourier Univ., Grenoble, 2011).
- [21] A. Goetschy and S.E. Skipetrov, *Phys. Rev. E* **84**, 011150 (2011).
- [22] A. Goetschy and S.E. Skipetrov, *EPL* **96**, 34005 (2011).
- [23] S. John, *Phys. Rev. Lett.* **53**, 2169 (1984).
- [24] P.W. Anderson, *Phil. Mag. B* **52**, 505 (1985).
- [25] S. John, *Phys. Today* **44**(5), 32 (1991).
- [26] M. Rusek, A. Orłowski, and J. Mostowski, *Phys. Rev. E* **53**, 4122 (1996).
- [27] F.A. Pinheiro, M. Rusek, A. Orłowski, and B.A. van Tiggelen, *Phys. Rev. E* **69**, 026605 (2004).
- [28] E. Akkermans, A. Gero, and R. Kaiser, *Phys. Rev. Lett.* **101**, 103602 (2008).
- [29] E. Abrahams, P.W. Anderson, D.C. Licciardello, and T.V. Ramakrishnan, *Phys. Rev. Lett.* **42**, 673 (1979).
- [30] J. Wang and A.Z. Genack, *Nature* **471**, 345 (2011).